

Emulating the logistic map with totalistic cellular automata

Franco Bagnoli^{1,2,3}

¹Department of Physics and Astronomy, University of Florence and CSDC, via G. Sansone, 1, Sesto Fiorentino, 50019, (FI), Italy.

²INFN, Sect. Florence.

³Espace-Dev, University of Perpignan via Domitia, 52 Avenue Paul Alduy Perpignan, 66000 France.

Contributing authors: franco.bagnoli@unifi.it;

Abstract

We investigate the conditions under which the mean-field formulation of a probabilistic, totalistic cellular automaton can approximate the logistic equation. We obtain that this goal can be obtained only for infinite-range neighborhood. We then performed simulations of the resulting one-dimensional probabilistic cellular automata, showing that this mean-field approximation is clearly obtained by shuffling the configuration, but also rewiring a fraction of links, either at each time or using the same randomization once and for all, in the spirit of the “small-world” mechanism. We show that it is possible to obtain a good approximation of the logistic behavior with a fraction of rewired links of 50% or more. We also show that there is a bifurcation cascade as a function of the rewired link, and this scenario also holds for a deterministic, totalistic CA with the same basic symmetries of the probabilistic one.

Keywords: Logistic map, totalistic cellular automaton, small-world effect

1 Introduction

The logistic map [1] is an extremely popular subject of research, Google Scholar reports more than 2 millions entries searching with this term.

This discrete-time dynamical system has been introduced by Robert May in 1976 (although a similar equation was already studied by E. Lorenz in 1964 [2]) as a model

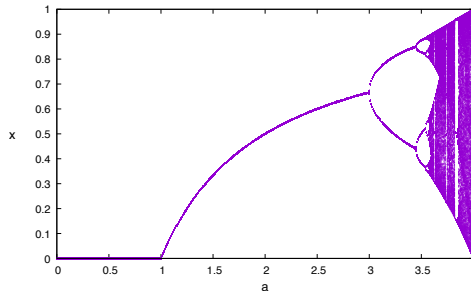


Fig. 1 Bifurcation diagram of the logistic map.

of the growth of a bounded population with discrete generations, as happens for insects that during the fall (autumn) lay eggs that will hatch the next spring.

The idea is that for a vanishing number of animals and large abundance of food, each insect will lay many eggs, and this induces an initial exponential growth. However, when the number of insects becomes large, the share of food will imply a smaller average number of eggs.

Neglecting spatial correlations, and assuming non-overlapping generations, at the end we get the equation

$$x' = ax(1 - x), \quad (1)$$

where $x \equiv x(t)$, $x' \equiv x(t + 1)$ and $0 \leq x \leq 1$ is proportional to the maximum number of insects, while $0 \leq a \leq 4$ is the control parameter.

As noted already in the title of May's work [1], by varying a we get an interesting bifurcation diagram for the long-time values of x , as shown in Fig. 1.

It is, therefore, natural to investigate which kind of microscopic models can give origin to a macroscopic dynamics equivalent to that of the logistic map. A similar problem has been addressed in Ref. [3], and the conclusions are that some two-dimensional Boolean cellular automata, coupled with random scattering of site values (random walks of individuals) and increasing neighborhood size, can effectively give origin to behavior of the average "density" of ones similar to that of the logistic map.

Indeed, Eq. (1) is a kind of mean-field description, and, therefore, in order to have collective "chaos" (i.e., an irregular behavior of the average density), one needs to randomize the population and destroy local correlations, for instance using a shuffling procedure [4], otherwise one gets patches of incoherent oscillations, as already noticed by Boccaro et al. [5]. In particular, we shall come back to the results of Ref. [4] at the end of Section 4.

However, the shuffling of a configuration is a process that is difficult to control, in the sense that it is not easy to impose a given degree of randomness. We can instead choose at random the neighbors of each cell, a procedure which is much easier to control, as illustrated in Section 2.

Moreover, we can profit of the "small-world effect". As noted by Watts and Strogatz [6], by rewiring a fraction of links of an otherwise local model, one can get a smooth transition to a system with mean-field properties. Indeed, as shown in models ranging from cellular automata [7, 8] to the parallel Ising model [9], this

rewiring procedure is another way to promote bifurcations in models whose mean-field approximation is a chaotic map.

The structure of this paper is the following. In Section 2 we define precisely the shuffling and rewiring procedures and the details of a totalistic, probabilistic cellular automaton. In Section 3 we shall obtain the conditions for which the mean-field description of such a model corresponds to the logistic map. In the same section we shall find that, as already noticed in Ref. [3], only for an infinite size of the neighborhood one can obtain the full range of the logistic map parameter. In Section 4 we shall present an implementation of a one-dimensional version of the previous cellular automaton, with different approaches to the mean-field behavior: shuffling the configuration, sampling at random the neighborhood at each time step, or rewiring a part of it only at beginning. We show that the resulting behaviors coincide, approximating that of the logistic map with finite-size noise. In the same section we shall study the bifurcation diagram of probabilistic and deterministic cellular automata induced by different levels of rewiring.

Finally, conclusions are drawn in the last section.

2 The cellular automaton model

We are interested in totalistic cellular automata of size N and neighborhood size R . We denote by $s_i(t) \in \{0, 1\}$ the value the cell i at time t . We shall use the abbreviation $s_i \equiv s_i(t)$ and $s'_i \equiv s_i(t+1)$. The whole configuration will be denoted as \mathbf{s} .

In order to define the problem, let us consider the adjacency matrix

$$c_{ij} = \begin{cases} 1 & \text{if } s'_i \text{ depends on } s_j, \\ 0 & \text{otherwise.} \end{cases}$$

The input connectivity of cell i is given by $\sum_j c_{ij}$ and we impose that all cells have the same input connectivity R (each row of c_{ij} has exactly R ones and $N - R$ zeros). The set of cells for which $c_{ij} = 1$ is called the neighborhood of cell i .

The totalistic character of the automaton corresponds to the fact that s'_i is a function of the sum of the values of the cells in its neighborhood at time t . We shall denote this sum by

$$v_i = \sum_j c_{ij} s_j \quad \text{with} \quad 0 \leq v_i \leq R.$$

Let us define the transition probabilities $\tau(k) \equiv \tau(1|k)$ which gives the probability that $s'_i = 1$ if $v_i = k$. The evolution of the cellular automaton is given by the parallel application of the same local rule

$$s'_i = f(\tau(v_i)),$$

where $f(x)$ takes value 1 with probability x and zero otherwise. For a deterministic cellular automaton, $\tau(k)$ are either zero or one and f is the identity.

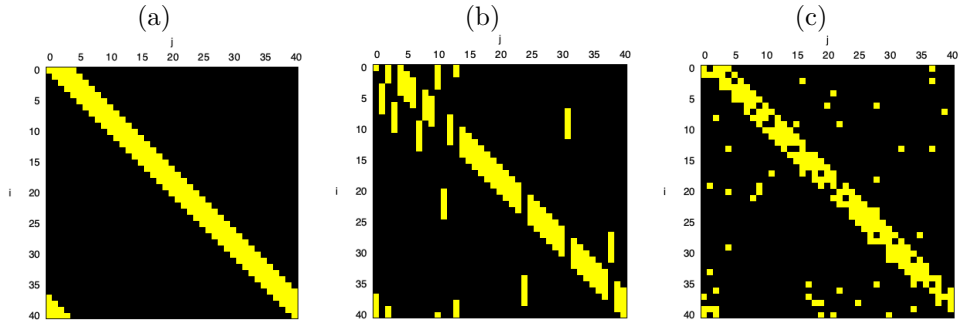


Fig. 2 Adjacency matrix for $N = 41$, $R = 5$, yellow dots marks connected neighbors. (a) Regular network (skewed); (b) shuffled $p \simeq 0.2$; (c) rewired $p \simeq 0.2$.

In the case of a uniform lattice, the matrix c is circulant, i.e., row $i + 1$ is obtained circularly shifting row i by one position.

Notice that for quantities computed on the configuration at the same time, like the density

$$x(t) = \frac{1}{N} \sum_i s_i(t) \quad (2)$$

it is irrelevant if we circularly shift all the rows of the matrix c of the same amount. As an example, let us assume that cell i depends on cells $i - 1$, i , and $i + 1$. Quantities computed at the same time take the same value if we instead make cell i depend on cells i , $i + 1$, $i + 2$ or any other set of three consecutive cells, provided that the same shift applies to all cells.

From now on, we shall consider one-dimensional automata, even if the same reasoning can be applied to higher dimensions with small modifications.

For a cellular automaton with local interactions, the matrix c is a band matrix. For row i we can take the lower bandwidth to be i and the upper bandwidth to be $i + R - 1$, with periodic boundary conditions, see Fig. 2-a for $N = 41$ and $R = 5$. Let us denote this matrix as $c_{ij}^{(r)}$.

The mean-field approximation consists in neglecting all spatial correlations, so that the evolution for the density x becomes

$$x' = \sum_{k=0}^R \binom{R}{k} \tau(k) x^k (1-x)^{R-k}, \quad (3)$$

since for an uncorrelated configuration, the probability of having k ones and $R - k$ zeros in the neighborhood of a cell is given by $x^k (1-x)^{R-k}$ times the number of possible permutations (the binomial coefficient).

There are at least two ways of actually destroying correlations in a configuration: either shuffling it or rewiring incoming links.

Let us examine the shuffling case. The basic procedure is the swapping of the values of two cells, say with indices j and k , at time t . Cells that at time $t + 1$ depended on

cell j now depend on cell k and vice versa. This is equivalent to swapping columns j and k in the matrix c , see Fig. 2-b.

In the rewiring case, we simply swap a number of entries in some rows of c , see Fig. 2-c. In both cases, the input connectivity (the sum of entries in each row) remains the same.

This procedure allows to quantify the degree p of randomization of the matrix c : it is given by the number of entries that are different from the regular case, divided by N and R :

$$p = \frac{1}{NR} \sum_{ij} |c_{ij}^{(r)} - c_{ij}|.$$

In the rewiring case, it is easy to generate matrices with a desired value of p , since one can simply assign a link to its regular position with probability $1 - p$ or to a random position outside the band with probability p . For the shuffling case, one can swap columns as far as the resulting value of p is less than the desired one (this procedure can take a long time for $p \simeq 1$).

The above described procedures can be performed at each time step (regenerating the matrix c), or just once at the beginning (keeping the same c). We shall refer to the first case with the term “annealed” and to the second with the term “quenched”. As we shall see, the results of the quenched and the annealed procedures are essentially the same for large lattices, which is essentially the small-world effect [6].

3 The approximation of the logistic map

Our goal is that of choosing the transition probabilities $\tau(k) \equiv \tau(1|k)$ so that Eq. (3) coincides with the logistic one, Eq. (1), with $0 \leq a \leq a_M$, possibly with $a_M = 4$.

Therefore, we want to compute $\tau(k)$ so that

$$\sum_{k=0}^R \binom{R}{k} \tau(k) x^k (1-x)^{R-k} = ax(1-x). \quad (4)$$

We can obtain a series of relationships. First of all, since the logistic map is invariant with respect to replacement of x with $1 - x$, we get

$$\tau(k) = \tau(R - k). \quad (5)$$

Setting $x = 0$ we get $\tau(0) = 0$ and, therefore, also $\tau(R) = 0$. We can obtain another relation by setting $x = 1/2$:

$$\frac{1}{2^R} \sum_{k=1}^{R-1} \binom{R}{k} \tau(k) = \frac{a}{4}. \quad (6)$$

We now proceed by equating the coefficients of the powers of x . Let us denote them by $b(k)$,

$$\sum_{k=1}^{R-1} \binom{R}{k} \tau(k) x^k (1-x)^{R-k} = \sum_{k=1}^{R-1} b(k) x^k,$$

in order to fulfill Eq. (4), we need to have

$$\begin{cases} b(1) = a, \\ b(2) = -a, \\ b(k) = 0 \quad \text{for } k \geq 3. \end{cases}$$

By expanding the binomial coefficients we get, for the coefficient $b(1)$,

$$b(1) = R\tau(1) = a$$

and, therefore,

$$\tau(1) = \frac{a}{R}.$$

The coefficient of x^2 comes from

$$\binom{R}{1} \tau(1) x (1-x)^{R-1} + \binom{R}{2} \tau(2) x^2 (1-x)^{R-2},$$

i.e., taking the second term from the expansion of the coefficients of $\tau(1)$ and the first from that of $\tau(2)$,

$$-R[R-1]\tau(1) + \frac{R(R-1)}{2}\tau(2) = -a$$

(where we indicated by square bracket the contribution coming from the expansion of $(1-x)^{R-k}$). Therefore,

$$\tau(2) = \frac{2(R-2)}{R(R-1)}a.$$

For the coefficient $b(3)$,

$$R \left[\frac{(R-1)(R-2)}{2} \right] \tau(1) - \frac{R(R-1)}{2} [R-2] \tau(2) + \frac{R(R-1)(R-2)}{3!} \tau(3) = 0;$$

and replacing the values of the computed τ , we get

$$\frac{(R-2)}{2} ((R-1) - 2(R-2))a + \frac{R(R-1)(R-2)}{3!} \tau(3) = 0.$$

After simplifying, the final expression is

$$\tau(3) = \frac{3(R-3)}{R(R-1)}a.$$

The procedure is similar for the other coefficients, and after some algebra, we obtain

$$\tau(k) = \frac{k(R-k)}{R(R-1)}a,$$

which actually holds for all k . Notice that this expression reflects the symmetry of Eq. (5).

We can check that the transition probabilities also satisfy Eq. (6). By considering the expansion of the binomial

$$\sum_{k=0}^R \binom{R}{k} x^k y^{R-k} = (x+y)^R,$$

we see that

$$xy \frac{\partial^2}{\partial x \partial y} \sum_{k=0}^R \binom{R}{k} x^k y^{R-k} = \sum_{k=0}^R \binom{R}{k} k(R-k) x^k y^{R-k} = R(R-1)xy(x+y)^{R-2},$$

so that, setting $x = y = 1/2$ and rearranging a bit, we get Eq. (6):

$$\frac{1}{2^R} \sum_{k=1}^{R-1} \binom{R}{k} \tau(k) = \frac{1}{2^R} \sum_{k=0}^R \binom{R}{k} \frac{k(R-k)}{R(R-1)} a = \frac{a}{4}.$$

The problem of approximating the logistic equation is now that of determining R such that the coefficients $\tau(k)$ are probabilities, i.e., between 0 and 1, which also establishes a maximum value $a_M(R)$.

For a given R the expression

$$\tau(k) = \frac{k(R-k)}{R(R-1)}a$$

is a discretized parabola, with a maximum for $k = R/2$ (we can consider R even for simplicity). Equating it to one, we get

$$a_M = 4 \frac{R-1}{R},$$

so that we cannot really have $a_M = 4$ for finite R , i.e., $a_M(R) < a_M(\infty) = 4$.

4 Cellular automaton bifurcation diagrams

Let us first consider the case $p = 1$, using the shuffling and rewiring methods, quenched or annealed. We can confirm that numerically we get the same results.

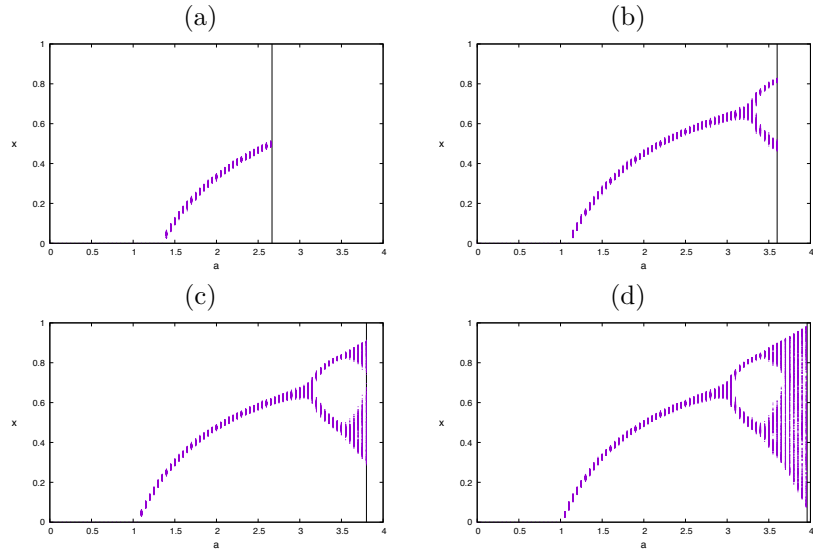


Fig. 3 Bifurcation diagrams of x for $0 \leq a \leq a_M$, $T = 100$ steps and lattice size $N = 10^4$, after a transient of 10^3 steps. The vertical line marks the value of a_M . The plots are the same for the shuffling, annealed and quenched procedure with $p = 1$. (a) $R = 3$; (b) $R = 10$; (c) $R = 20$ and (d) $R = 100$.

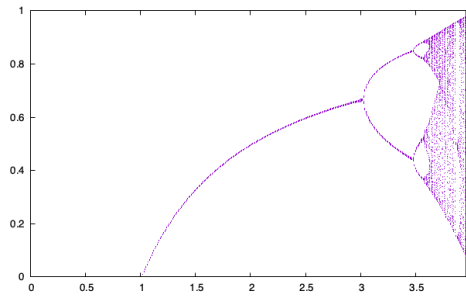


Fig. 4 Bifurcation diagrams of the density x for $0 \leq a \leq a_M = 0.96$, $R = 100$ and quenched rewiring, $T = 100$ steps and lattice size $N = 10^6$, after a transient of 10^3 steps. The vertical line marks the value of a_M .

As shown in Fig. 3, the plot of the average density x starts resembling the bifurcation diagram of the logistic map as R increases, with a noise due to the finite size N of the lattice.

Actually, the bifurcation diagram of the disordered cellular automaton approaches more and more that of the logistic map by increasing the lattice size. In Fig. 4 the same diagram of Fig. 3-d is shown, for $N = 10^6$.

It is now interesting to examine how the small-world procedure (quenched rewiring the incoming neighborhood links with probability p) modulates the approach to the logistic equation.

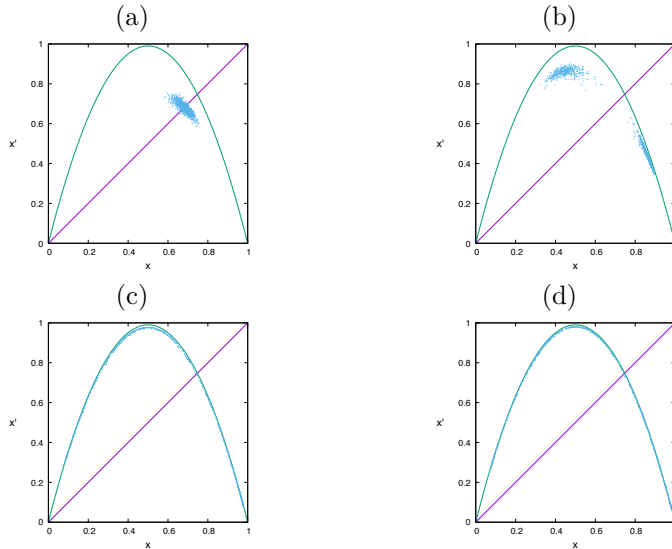


Fig. 5 Plot of the logistic map for $a = a_M = 3.96$ and the return map $x' \equiv x(t+1)$ vs $x \equiv x(t)$ for $R = 100$, $T = 1000$ steps and lattice size $N = 10000$, after a transient of 100000 steps. (a) $p = 0.1$; (b) $p = 0.2$; (c) $p = 0.5$ and (d) $p = 1.0$.

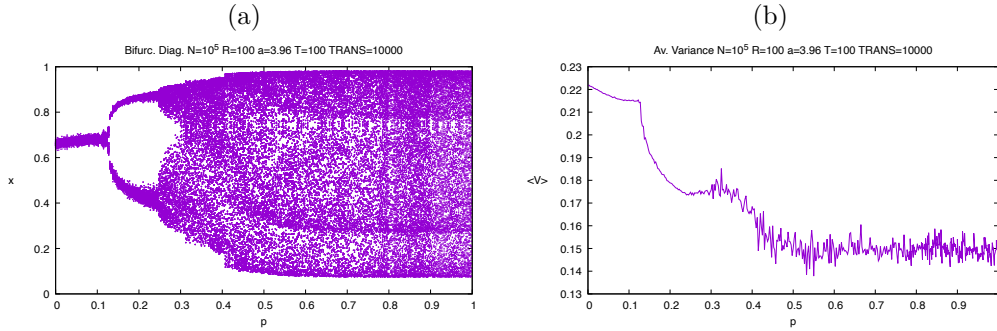


Fig. 6 (a) The bifurcation diagram of the density x vs the rewiring probability p . (b) The average variance of the configuration $\langle V \rangle = (1/T) \sum_t V(s(t)) = (1/T) \sum_t x(t)(1-x(t))$ vs rewiring probability p . Parameters: $R = 100$, $a = a_M = 3.96$, $T = 100$ steps and lattice size $N = 10^5$, after a transient of 10^4 steps.

One can see from Fig. 5 that for small values of p the density is essentially constant, even for the maximum value $a = a_M$. Indeed, for a local neighborhood, the system is practically decoupled into almost independent domains, which oscillate in an incoherent way. By increasing p the return map approaches the logistic curve.

By looking at Fig. 6-(a), it is evident that the range of x already approximates the final one for $p \simeq 0.5$ (even if there are other structures appearing for larger values of p), for the maximum value of a .

One can directly check the bifurcation diagrams for various values of the rewiring parameter p , as shown in Fig. 7. One can see that near $a = a_M$ the main bifurcation

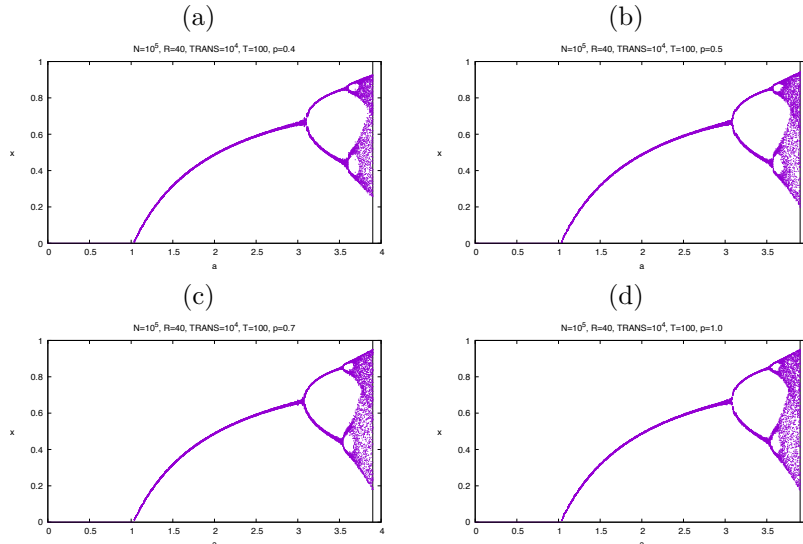


Fig. 7 The bifurcation diagram of the density x vs the parameter a for various values of p and $N = 10^5$, $R = 40$, $T = 100$ after a transient of 10^4 steps. (a) $p = 0.4$; (b) $p = 0.5$; (c) $p = 0.7$; (d) $p = 1.0$. The vertical line marks the value of $a_M = 3.9$.

locations are almost already established for $p \geq 0.5$, while far from the maximum value of a the agreement is excellent also for smaller p . Clearly, more details may emerge by increasing the lattice size, as shown in Fig. 4.

The small-world transition of Figs. 5 and 6 can be interpreted as a synchronization process: the density x can oscillate in a quasi-deterministic way instead of fluctuating around an average value only if the sites in the configuration are coherent (have similar values for many neighborhoods). However, since each site value can only assume values 0 and 1, intermediate values of x are possible only if large portions of the configuration take different values. So the maximum coherence is for x near zero or one.

For Boolean variables, the variance $V(\mathbf{s})$ of configuration \mathbf{s} is

$$V(\mathbf{s}) = \frac{1}{N^2} \left(N \sum_i s_i^2 - \left(\sum_i s_i \right)^2 \right) = x(\mathbf{s})(1 - x(\mathbf{s})),$$

where x is the density defined in Eq. (2), since $s_i^2 = s_i$. This implies that the smallest values of the variance correspond to the extreme values of the density x . In the numeral simulations, the variance is averaged over time for a certain number of steps.

Another way of looking at the bifurcation diagram of Fig. 6 is that of increasing synchronization. Indeed, the variance of the configuration averaged over time, Fig. 6-(b), shows a steep decrease in correspondence of the first bifurcation (appearance of a limit cycle) for $p \simeq 0.2$, and stabilizes at its minimum value for $p \geq 0.5$, where indeed the distribution approaches the final one, see Fig. 5-(c) and (d).

The bifurcation diagram induced by randomization can be appreciated also for deterministic cellular automaton, which have no continuous adjustable parameters.

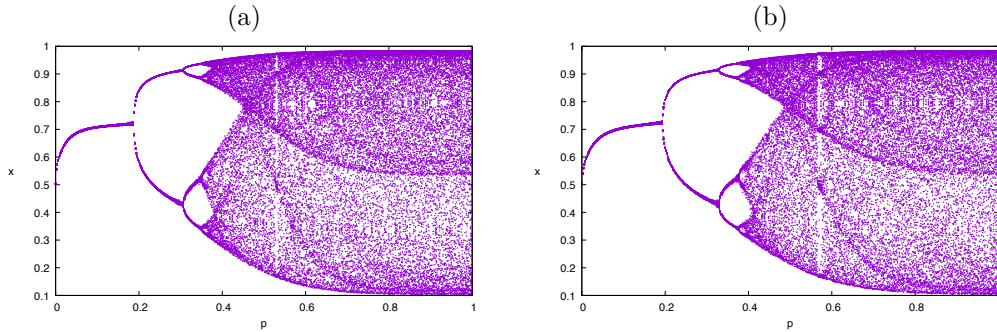


Fig. 8 Bifurcation diagram of the $R = 7$ totalistic cellular automata rule 126. $T = 100$ steps of the density x as a function of the rewiring fraction p for $N = 10^6$. (a) Annealed version, links are rewired at each time steps, transient of 10^3 steps; (b) quenched version, links are rewired only at beginning and kept fixed, transient of $2 \cdot 10^3$ steps.

This has been done by Boccaro and Roger for some totalistic cellular automata using a shuffling procedure [4].

In particular, let us investigate the totalistic case $R = 7$, with transition “probabilities” (actually deterministic) such that

$$s'_i = \begin{cases} 0 & \text{if } k = 0 \text{ or } k = 7, \\ 1 & \text{otherwise.} \end{cases}$$

Since the result of this rule for $k = 7, 5, \dots, 0$ is $0, 1, 1, 1, 1, 1, 0$, i.e., 126 in base-two representation, this rule can be identified by this number. Notice that this deterministic automata obeys the requirements of Eq. 5 and $\tau(0) = \tau(R) = 0$.

The relative mean-field equation is

$$x' = x(1-x)[7(1-2x+3x^2-2x^3+x^4)]$$

and one can see that this map has the structure of the logistic map, with a quadratic maximum for $x = 1/2$. It is not surprising that the density of the related microscopic model can exhibit a bifurcation diagram similar to that of the logistic map when approaching the mean-field behavior [4], as suggested by the universality of chaos mechanisms [10].

This model is also a good testbed for the small-world hypothesis. Indeed, one can see in Fig. 8 that the bifurcation diagram of rule 126 as a function of the disorder p shows several period-doubling and intermittent bifurcations, and that quenched and annealed rewiring give similar results, with small differences in the location of the bifurcation points. The annealed approximation is much more demanding in computational terms.

As for the probabilistic case, for the regular lattice the dynamics is “chaotic” at the microscopic level, so that distant patches are uncorrelated and the average density is about $1/2$. The shuffling or rewiring of lattice behaves as a spatial homogenization mechanism, so that the density of the configuration starts oscillating following the

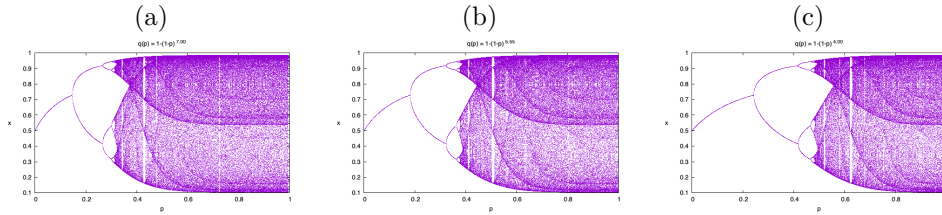


Fig. 9 The bifurcation diagram of the map of Eq. (7) for $q(p) = 1 - (1-p)^y$, with (a) $y = 7$; (b) $y = 5.55$; (c) $y = 4$.

mean-field equation and one has a transition between microscopic to macroscopic chaos.

One can try to approximate this transition by assuming that the dynamics of the density is given by a combination of the “chaotic” value of the density, $x = 1/2$, and that of the mean field, i.e.,

$$x' = (1 - q(p))\frac{1}{2} + q(p)x(1 - x)[7(1 - 2x + 3x^2 - 2x^3 + x^4)], \quad (7)$$

with $q(p)$ being an appropriate function of p . For a given site, the neighborhood coincides to that of the regular lattice if no links had been rewired, and this happens with probability $(1-p)^R$, so the “weight” of the mean-field contribution should in principle be $q(p) = 1 - (1-p)^y$, with $y = R = 7$. As shown in Fig. 9, one obtains a bifurcation diagram more similar to the experimental one (for what concerns the localization of bifurcations) for $y = 5.55$.

5 Conclusions

We have obtained the conditions for the transition probabilities of a totalistic cellular automaton to approximate, in the mean-field limit, the logistic equation, and shown that this is a task that can be accomplished only in the limit of infinite-range neighborhood.

We have then shown that, exploiting the Watts-Strogatz “small-world” mechanism, one can actually obtain a good approximation of the logistic behavior with a one-dimensional cellular automaton already with a fraction of rewired links of about 50% for the maximum value of the parameter a . This results holds also for smaller values of a .

We have also investigated the bifurcation cascade as a function of the rewired link, and shown that this scenario also holds for a deterministic, totalistic CA with the same basic symmetries of the probabilistic one, with either a random choice of neighbors at each time, or a quenched (small-world) connection matrix.

Declarations

- Funding: not applicable
- Conflict of interest/Competing interests: not applicable

- Ethics approval and consent to participate: not applicable
- Consent for publication: not applicable
- Data availability: not applicable
- Materials availability: not applicable
- Code availability: simulation codes are available upon request
- Author contribution: only one author

References

- [1] May, R.M.: Simple mathematical models with very complicated dynamics. *Nature* **261**(5560), 459–467 (1976) <https://doi.org/10.1038/261459a0>
- [2] Lorenz, E.D.: The problem of deducing the climate from the governing equations. *Tellus A: Dynamic Meteorology and Oceanography* **16**(1), 1–11 (1964) <https://doi.org/10.3402/tellusa.v16i1.8893>
- [3] Dzwiniel, W.: Spatially extended populations reproducing logistic map. *Central European Journal of Physics* **8**(1), 33–41 (2010) <https://doi.org/10.2478/s11534-009-0089-6>
- [4] Boccara, N., Roger, M.: Period-doubling route to chaos for a global variable of a probabilistic automata network. *Journal of Physics A: Mathematical and General* **25**(16), 1009–1014 (1992) <https://doi.org/10.1088/0305-4470/25/16/004>
- [5] Boccara, N., Roblin, O., Roger, M.: Automata network predator-prey model with pursuit and evasion. *Physical Review E* **50**(6), 4531–4541 (1994) <https://doi.org/10.1103/physreve.50.4531>
- [6] Watts, D.J., Strogatz, S.H.: Collective dynamics of ‘small-world’ networks. *Nature* **393**(6684), 440–442 (1998) <https://doi.org/10.1038/30918>
- [7] Bagnoli, F., Rechtman, R.: Topological bifurcations in a model society of reasonable contrarians. *Physical Review E* **88**(6) (2013) <https://doi.org/10.1103/physreve.88.062914>
- [8] Bagnoli, F., Rechtman, R.: Bifurcations in models of a society of reasonable contrarians and conformists. *Physical Review E* **92**(4) (2015) <https://doi.org/10.1103/physreve.92.042913>
- [9] Bagnoli, F., Rechtman, R.: Stochastic bifurcations in the nonlinear parallel Ising model. *Physical Review E* **94**(5) (2016) <https://doi.org/10.1103/physreve.94.052111>
- [10] Feigenbaum, M.J.: Universal behavior in nonlinear systems. *Physica D: Nonlinear Phenomena* **7**(1–3), 16–39 (1983) [https://doi.org/10.1016/0167-2789\(83\)90112-4](https://doi.org/10.1016/0167-2789(83)90112-4)